AD-A156 029 A PLANAR VERSION OF A 40 GIGAHERTZ REACTIVELY STEERED ADAPTIVE ARRAY(U) NAVAL WEAPONS CENTER CHINA LAKE CA R J DINGER MAR 85 NWC-TP-6621 SBI-AD-E900 451 1/1

UNCLASSIFIED F/G 9/1 NL

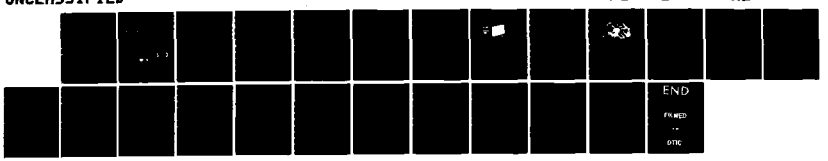

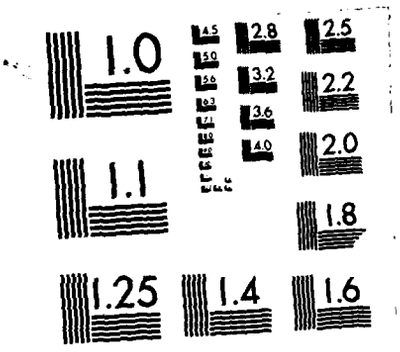

NWC TP 6621

A Planar Version of a 4.0 Gigahertz Reactively Steered Adaptive Array

by
Robert J. Dinger
Research Department

MARCH 1985

NAVAL WEAPONS CENTER
CHINA LAKE, CA 93555-6001

Naval Weapons Center
AN ACTIVITY OF THE NAVAL MATERIAL COMMAND

FOREWORD

Antenna arrays that operate at frequencies up to 6 gigahertz or so on air-launched guided missiles are necessarily compact because of limited space. Research has been in progress since fiscal year 1982 on a compact adaptive array that uses reactively loaded parasitic elements for pattern control. This report describes experimental results with a planar microstrip version of such an array. A companion to this report is Naval Weapons Center TP 6611, "A Simulation Study of Jammer Nulling Trade-Offs in a Reactively Steered Adaptive Array." The research is part of a continuing effort to explore novel radio frequency radiating and receiving structures for applications to airborne communications and radar systems.

The research described in this report was performed during fiscal year 1984. It was supported primarily by the Office of Naval Research (Code 414), with additional funding from the Independent Research program of the Naval Weapons Center.

D. A. Bowling has reviewed this report for technical accuracy.

Approved by
E. B. ROYCE, Head
Research Department
8 March 1985

Under authority of
K. A. DICKERSON
Capt., USN
Commander

Released for publication by
B. W. HAYS
Technical Director

NWC Technical Publication 6621

Published by . . . . . Technical Information Department
Collation . . . . . Cover, 10 leaves
First printing . . . . . 120 copies

UNCLASSIFIED

SECURITY CLASSIFICATION OF THIS PAGE (When Data Entered)

REPORT DOCUMENTATION PAGE		READ INSTRUCTIONS BEFORE COMPLETING FORM
1. REPORT NUMBER NWC TP 6621	2. GOVT ACCESSION NO. AD-A156029	3. RECIPIENT'S CATALOG NUMBER
4. TITLE (and Subtitle) A Planar Version of a 4.0 Gigahertz Reactively Steered Adaptive Array		5. TYPE OF REPORT & PERIOD COVERED Interim report on continuing problem 6. PERFORMING ORG. REPORT NUMBER
7. AUTHOR(s) Robert J. Dinger		8. CONTRACT OR GRANT NUMBER(s)
9. PERFORMING ORGANIZATION NAME AND ADDRESS Naval Weapons Center China Lake, CA 93555-6001		10. PROGRAM ELEMENT, PROJECT, TASK AREA & WORK UNIT NUMBERS 61153N; 61152N
11. CONTROLLING OFFICE NAME AND ADDRESS Naval Weapons Center China Lake, CA 93555-6001		12. REPORT DATE March 1985 13. NUMBER OF PAGES 18
14. MONITORING AGENCY NAME & ADDRESS(if different from Controlling Office)		15. SECURITY CLASS. (of this report) UNCLASSIFIED 15a. DECLASSIFICATION/DOWNGRADING SCHEDULE

16. DISTRIBUTION STATEMENT (of this Report)

Approved for public release; distribution is unlimited.

17. DISTRIBUTION STATEMENT (of the abstract entered in Block 20, if different from Report)

18. SUPPLEMENTARY NOTES

19. KEY WORDS (Continue on reverse side if necessary and identify by block number)

Adaptive Arrays
Anti-jam Techniques
Optimization Techniques
Parasitic Antennas
Microstrip Antennas

20. ABSTRACT (Continue on reverse side if necessary and identify by block number)

See back of form.

DD FORM 1 JAN 73 1473 EDITION OF 1 NOV 65 IS OBSOLETE
S/N 0102-LF-014-6601

UNCLASSIFIED

SECURITY CLASSIFICATION OF THIS PAGE (When Data Entered)

(U) A Planar Version of a 4.0 Gigahertz Reactively Steered Adaptive Array, by Robert J. Dinger. China Lake, Calif., Naval Weapons Center, March 1985. 18 pp. (NWC TP 6621, publication UNCLASSIFIED.)

(U) A planar (two-dimensional) reactively steered adaptive array which includes a single active microstrip element and eight closely coupled parasitic microstrip elements has been designed and tested. Steering of a null towards a single incident jammer is accomplished by adaptive control of reactive terminations on the parasitic elements using a guided random search algorithm. The planar array can steer a null in both the elevation and azimuth directions with a depth of 30 decibels.

INTRODUCTION

Adaptive arrays reduce the energy of an incident jammer signal reaching a receiver by steering an antenna pattern null in the direction of the interference. The typical adaptive array employs a controllable complex weight on each array element, and the weighted element outputs are combined in an electronic summing element to obtain the array output. Even though the term "adaptive" implies some accommodation to imperfections in the array environment, it has been found that element spacings of 0.25λ (λ = wavelength) or less degrade seriously the depth of a null that an adaptive array can form toward a jammer, because of the mutual coupling between the elements (Reference 1).

This report presents results for a planar array, known as a reactively steered adaptive array (RESAA), that can maintain deep nulls toward a jammer even when the element spacing is as small as 0.1λ. A RESAA (Figure 1) has only a single element that is connected by a transmission line to a receiver. The remaining elements are parasitic, and the pattern is formed according to the values of the reactive terminations on these parasitic elements. The basic scheme of a reactively steered array was first proposed by Harrington for deterministic control (Reference 2); over the last several years, we have been applying this idea to adaptive arrays using a linear array of microstrip patch elements resonant at 4.0 gigahertz (References 3 through 6).

The earlier work employed linear arrays with a relatively small number of elements (usually five); the interested reader is referred to a series of three reports that describe these results (References 3 through 5). Herein, we present results on a planar array of nine elements arranged in a cross configuration. The goal of the planar RESAA is to steer a null in both azimuth and elevation. As in the earlier work, we use microstrip patch elements resonant at 4.0 gigahertz. Only a single incident jammer is present, with no desired signal, so that a power inversion algorithm with no signal sorting is used.

The extension of the experience with linear arrays to planar arrays is not as straightforward as one might think. The doubling of

the number of controlled loads (from four to eight) presents problems in convergence speed for a control algorithm using serial adjustment (as was used for the linear array). Hence, an algorithm using simultaneous adjustment of the loads (i.e., in parallel) is required.

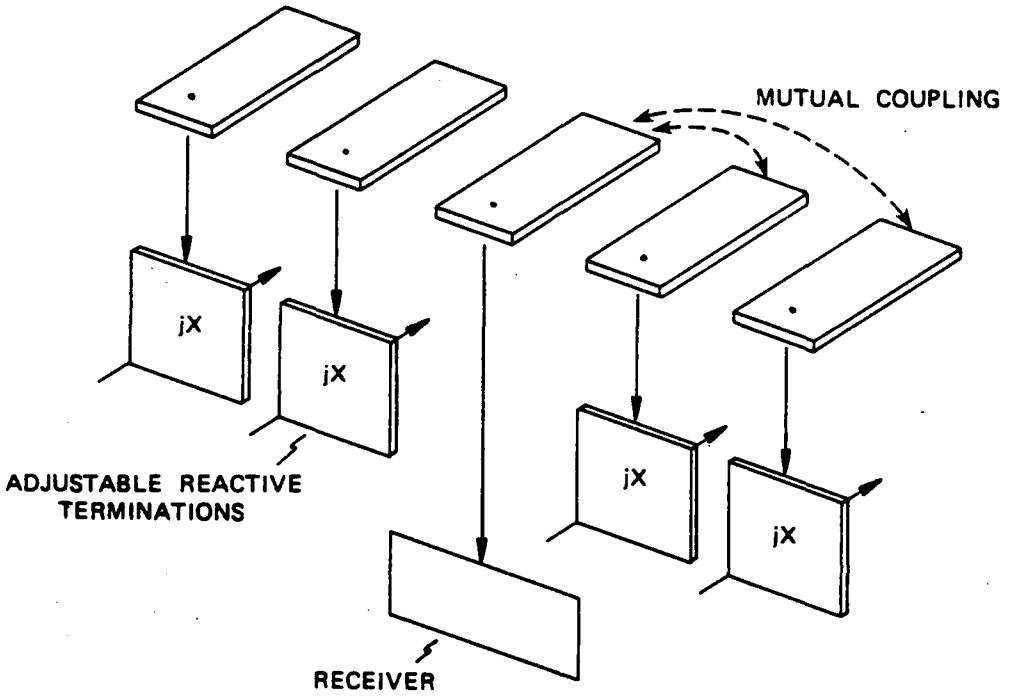

FIGURE 1. Reactively Steered Adaptive Array.

Below, we first describe the experimental array and the measurement configuration. We then give details of the control algorithms used to control the array, followed by the experimental results. Rather than repeat much of the theory of RESAA operation given in the earlier reports (References 3 through 5), we have summarized the theory in the Appendix.

ANTENNA DESIGN AND MEASUREMENT DETAILS

Figure 2 shows the five-by-five cross configuration of the array. The element at the cross intersection is connected to the receiver, and the other elements are terminated in reflection phase shifters. Each element is 1.0 × 2.33 centimeters; the adjacent edge and center-to-

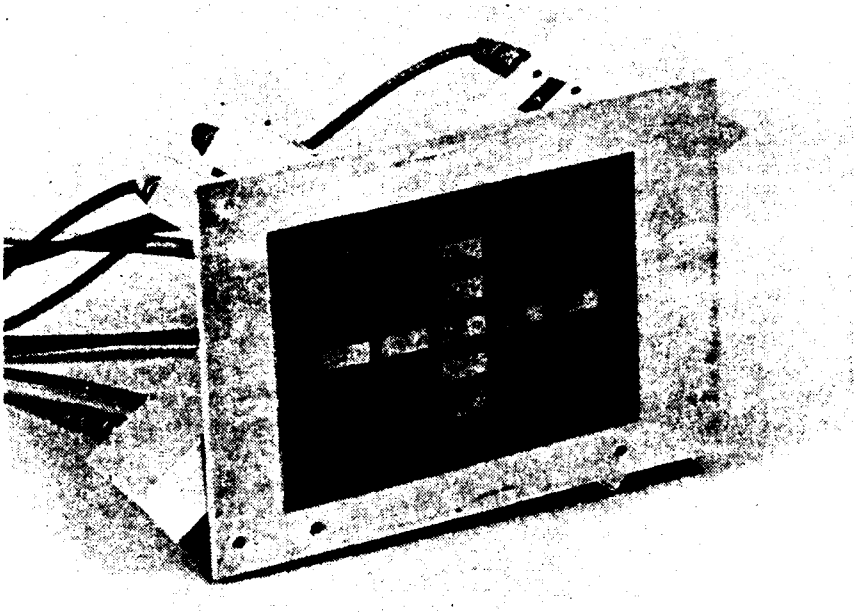

FIGURE 2. Planar Reactively Steered Adaptive Array.

center spacings are 0.1 and 0.23λ, respectively, in the H-plane, and 0.067 and 0.37λ, respectively, in the E-plane (see Figure 3). The elements are formed on Rexolite 1422 with a thickness of 1.58 millimeters and are resonant at 4.0 gigahertz.

Table 1 lists values of the couping coefficients between elements of the array. These numbers are the magnitude (in decibels) of the element S_{12} of the voltage scattering matrix.

TABLE 1. Mutual Coupling Values for Array in Figure 2.

The definitions of the E- and H-planes are shown in Figure 3.

Number of intervening elements	H-plane value of S_{12}, dB	E-plane value of S_{12}, dB
0 (Adjacent elements)	8.4	14.9
1 (Next nearest neighbors)	17.1	27.1
2	22.8	27.3
3	25.2	29.1

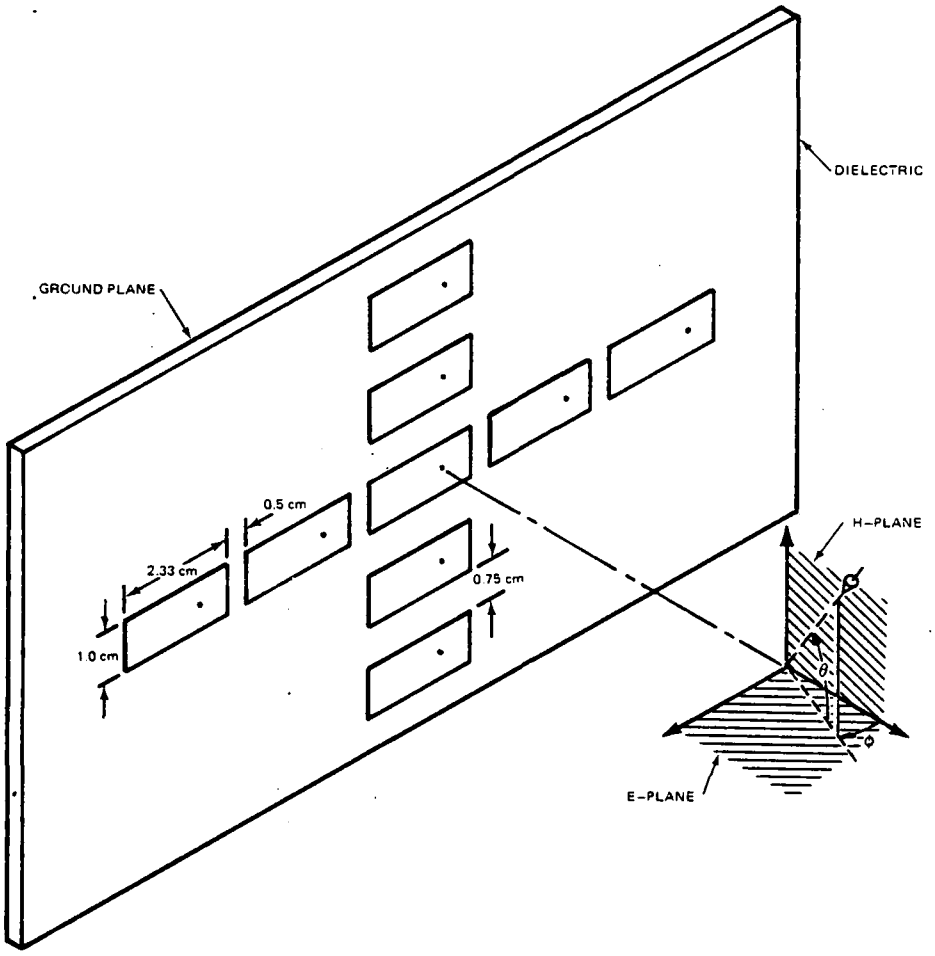

FIGURE 3. Diagram of Antenna Array Shown in Figure 2.

Figure 4 is a view of the back of the array. The reactive loads are varactor-diode reflection phase shifters identical to the design described in Reference 4. Approximately 250 degrees of phase shift can be obtained with a bias voltage range of 0 to -10 volts. The variation of the magnitude of the reflection coefficient for these loads over this bias voltage range was less than 1.0 decibel.

In Figure 5 we show the array configured for closed-loop operation on a rooftop test range. Only two of the eight varactor phase shifter reactive loads are indicated in the figure. The output of the array was passed directly to a Narda Model 7000A digital power meter. As a receiver, this power meter had several advantages: It had an extremely

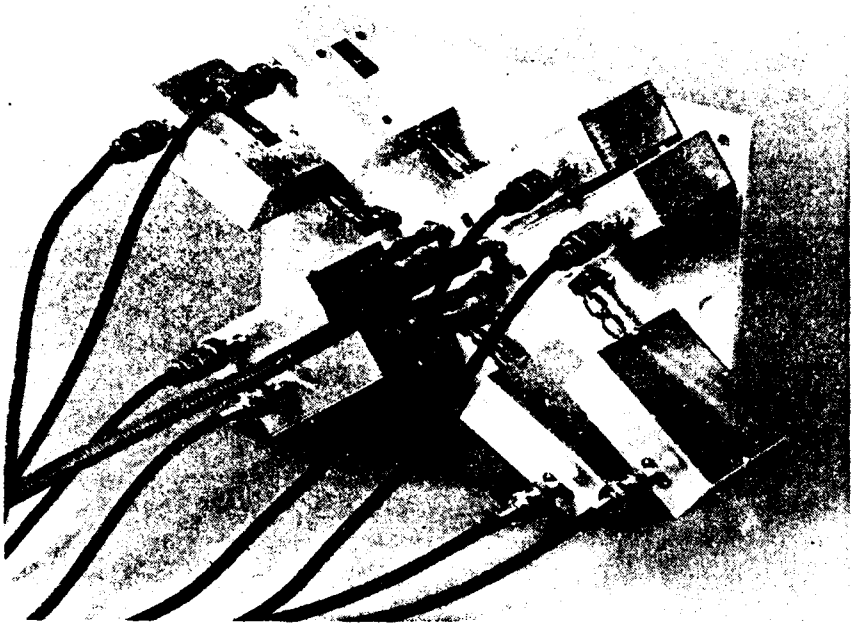

FIGURE 4. Rear View of Planar RESAA.

wide dynamic range (about 60 decibels), and a GPIB-488 bus output was available for interface to the computer. The power meter also had one disadvantage: To obtain the wide dynamic range and high accuracy, the meter had a 0.5-second integration time; hence, actual adaptation times were slow. All curves of transient response, below, are expressed in terms of number of iterations rather than seconds for this reason. Performance with an optimized communications receiver would, of course, be much faster than with the power meter.

To evaluate array performance, we positioned the array so that the signal from the horn antenna was incident at a given azimuth and elevation angle. We then allowed the nulling algorithm (described in the following section) to operate. When steady state conditions were reached, we froze the reactive load values and proceeded to measure the patterns, using the jamming signal as a pattern test source. To obtain the iso-power contour plots, we stepped the antenna array through the elevation and azimuth angles in a raster pattern; the values were printed on a grid, and we then drew the contours in by hand.

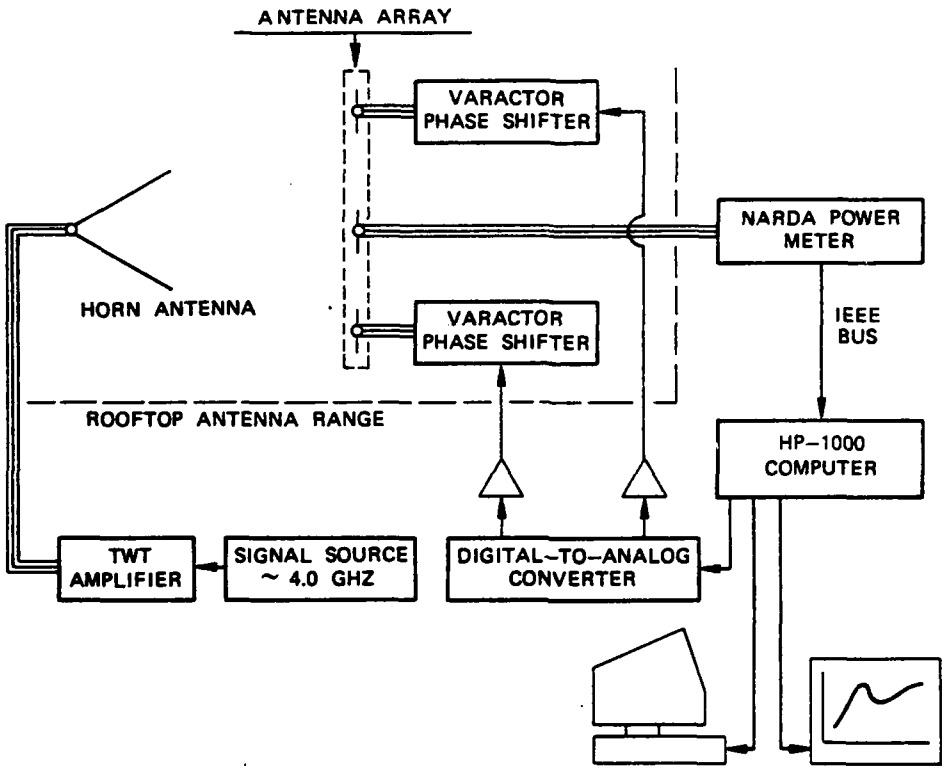

FIGURE 5. Test Setup.

CONTROL ALGORITHMS

REVIEW OF LINEAR ARRAY CONTROL TECHNIQUES

The control algorithm accepts the current value of the jammer power and then provides control signals to the reactive loads to attempt to decrease the jammer power further. The linear array control algorithms described in References 3 through 6 used a combination of two techniques: random search and steepest descent.

The random search phase came first and had the objective of selecting a starting point for the subsequent steepest descent technique. A series of load vectors $\vec{X}(m)$ (see the Appendix for a definition of $\vec{X}$) were generated according to

$$\vec{X}(m) = \vec{U}(m) \quad (m = 1...M) \tag{1}$$

in which $\vec{U}(m)$ is a vector of load values selected by a random number generator with uniform density over the 0- to -10-volt control range of the varactors. The index m denotes the iteration number. The values in $\vec{X}(m)$ were fed to the phase shifter terminations and the receiver output $\vec{V}(m)$ measured. At the end of the random search phase, for which typically M = 20 was used, the value of $\vec{X}$ for which $\vec{V}(m)$ was lowest then became the starting point for the steepest descent phase.

The steepest descent technique was a form of gradient search algorithm, in which corrections to each value of the reactive load were generated proportional to the slope of the error surface:

$$\vec{X}(j+1) = \vec{X}(j) - K\nabla\vec{V} \tag{2}$$

The quantity K is a positive constant that controls the convergence rate and is selected by stability considerations.

PLANAR ARRAY CONTROL TECHNIQUE

Random search is an example of a simultaneous load change method (all loads were changed at once), which required only a single measurement of received power for each iteration. Steepest descent is a sequential load change method (the loads can be changed only one at a time, in order to determine each component of the gradient), which required a measurement of receiver power for each individual change in load. Although steepest descent was the faster method for the linear array with four loads, it became very slow when an additional four elements were added to form the planar array. Hence, a variant of random search known as guided random search was used to control the planar RESAA (Reference 7).

In guided random search the value of $\vec{X}(j+1)$ is chosen according to

$$\vec{X}(j+1) = \vec{X}(j) + \vec{x}(j) \tag{3}$$

where $\vec{x}(j)$ is a vector whose components are selected from a Gaussian sequence with zero mean and variance σ. At each iteration, the components of $\vec{x}$ are derived from an appropriate Gaussian random number generator, the new values of $\vec{X}$ are entered simultaneously, and then only a single reading of the receiver output is made. If this choice of $\vec{x}(j)$ reduces the interference power, the new value of $\vec{X}$ is used as the starting point for the next iteration; otherwise, the old value of $\vec{X}$ is retained and a new trial $\vec{x}(j)$ is selected.

In most of our runs, we used guided random search, although we made some comparison runs using steepest descent control. The sequence standard deviation σ for best performance was selected by trial and error. A large value of σ causes a wide portion of the error surface $V(\vec{X})$ to be sampled and, hence, may find a minimum in the error surface that a small value of σ might overlook. However, if the error surface has a steep canyon-type minimum, a large value of σ might prevent convergence to the minimum. Figure 6 illustrates this point.

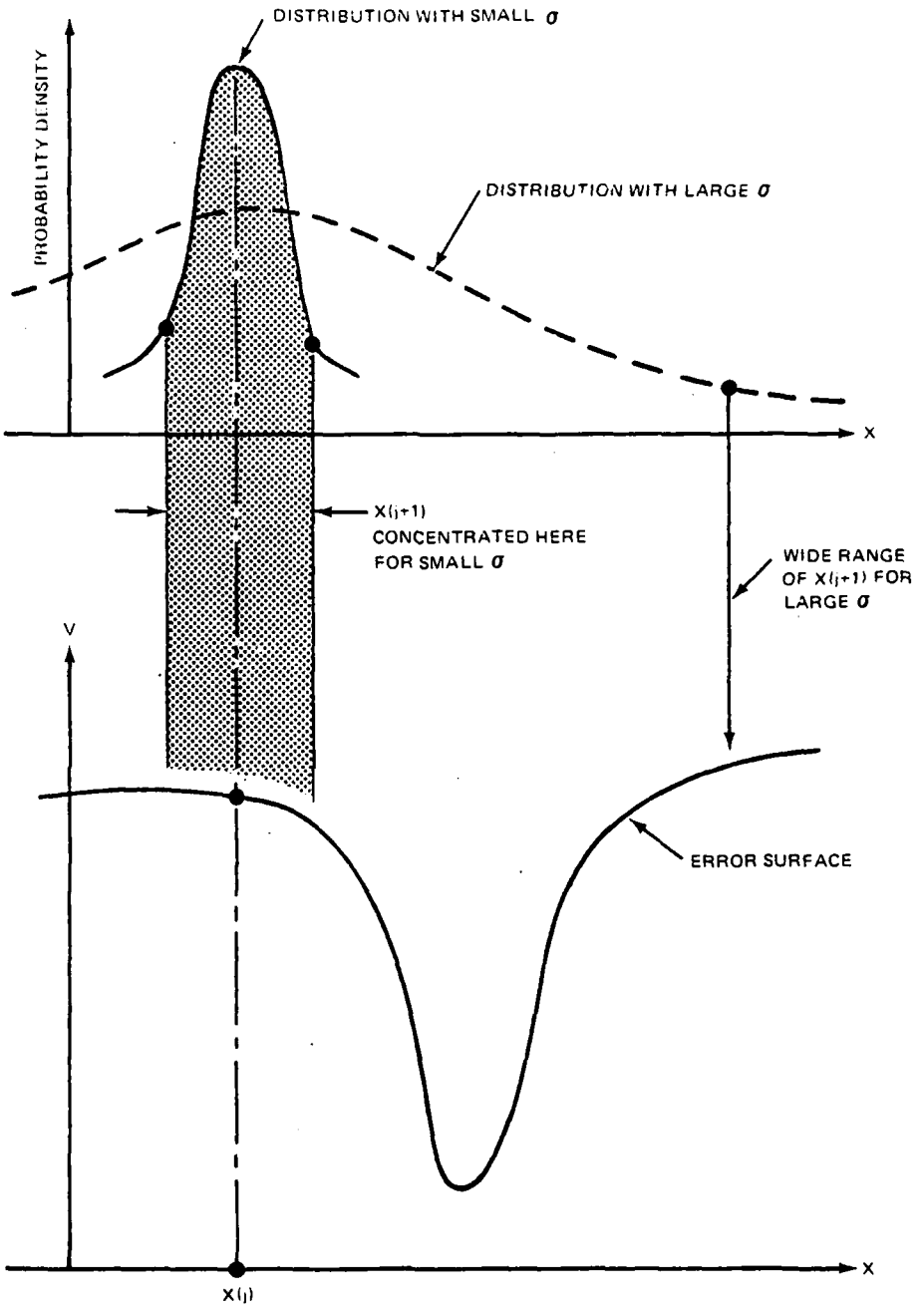

FIGURE 6. Illustration of Effect of Value of σ on Guided Random Search.

EXPERIMENTAL RESULTS

Figures 7 through 10 are the results of a typical run taken for a jamming source incident from an angle of 45 degrees in azimuth and 25 degrees in elevation. Figure 7 shows the received jammer power at each iteration, displaying the reduction in jammer power as the array adapts with guided random search control. Three curves are given for three different values of σ. For this run, a value of $\sigma = 0.15$ volt is clearly optimum; in general, this was found to be an optimum value for other conditions also. Figure 8 is a comparison transient response curve using steepest descent control. At first glance, it might appear that steepest descent is faster because only 40 iterations are needed, compared with 200 iterations for guided random search (Figure 7). However, as discussed above, each steepest descent iteration requires eight received power measurements (one for each load), compared with one measurement per iteration for guided random search. Hence, since the power measurement is by far the most time-consuming operation, guided random search is actually about 40% faster.

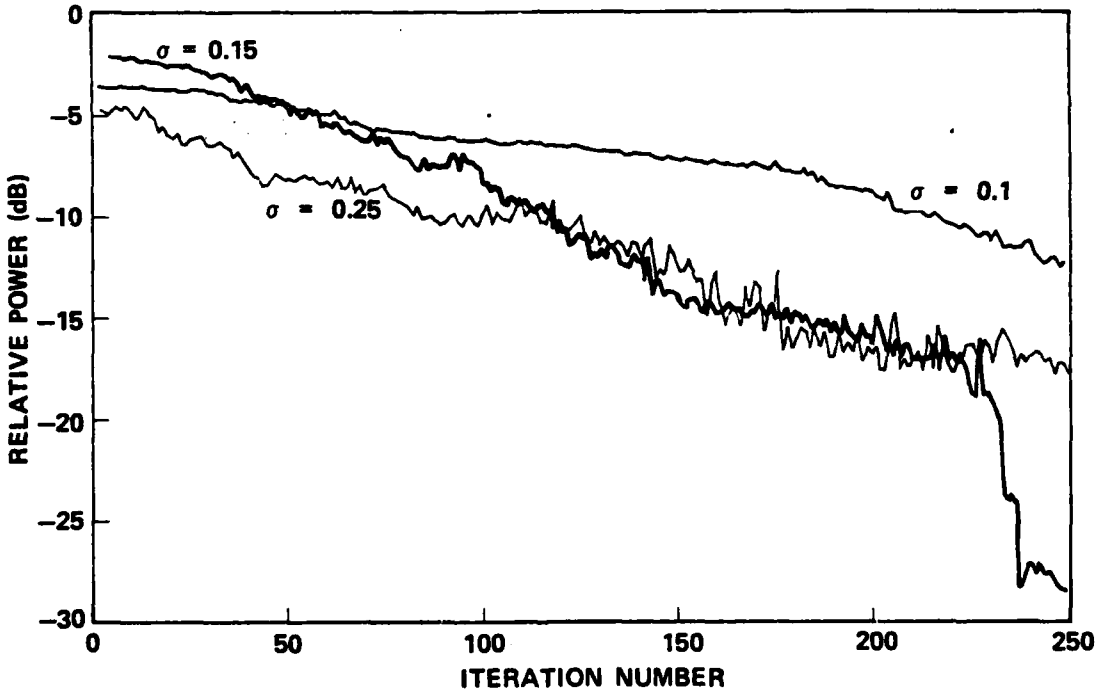

FIGURE 7. Reduction in Jammer Power During Guided Random Search Processing. Curves are shown for three different values of σ. The ordinate is given in decibels relative to the power received by a single isolated antenna element at element boresight ($\phi = \theta = 0$ degrees). Jammer incident at $\phi = 45$ degrees, $\theta = 25$ degrees.

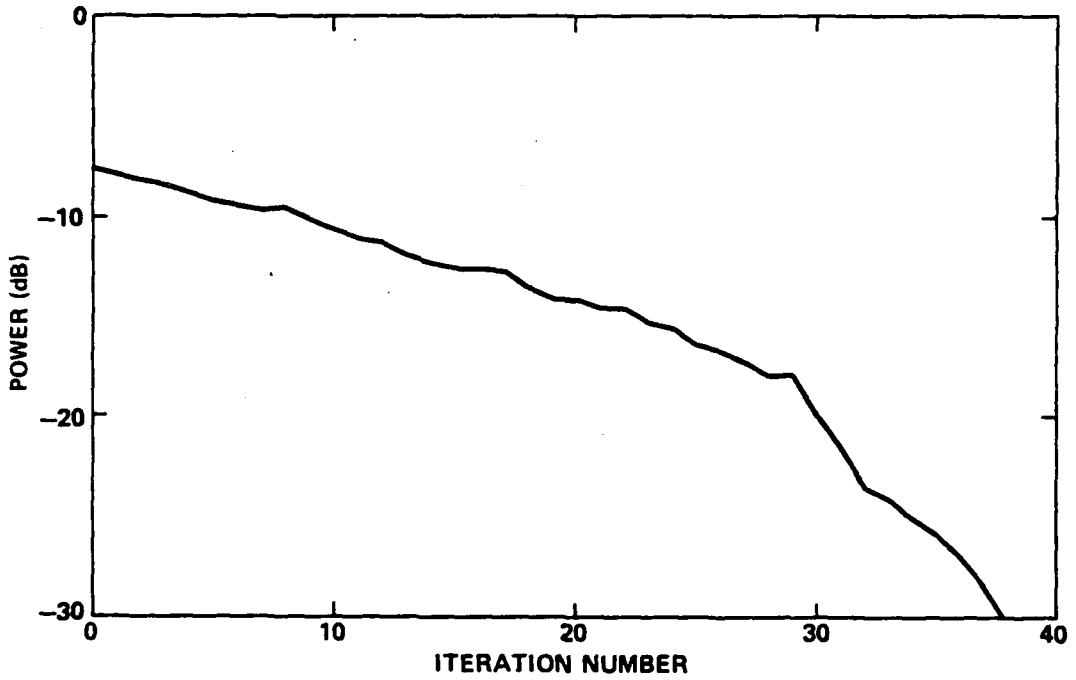

FIGURE 8. Reduction in Jammer Power During Steepest Descent Processing for Same Conditions as Figure 7.

Figure 9 is an iso-power contour plot of the null in a portion of the transverse plane. The significant point of this figure is the degree to which the null is well confined in both the azimuth and elevation directions, with a response 18 decibels above the null depth at angles only 15 degrees from the null position. The elongation of the contours in the elevation direction results from the smaller mutual coupling between the elements in the E-plane (see Figure 1), a phenomenon that is even more apparent in another pattern given below (Figure 12). In Figure 10 we show antenna patterns for Figure 9 at two cuts.

Figure 11 is another example of the transient response for a jammer incident at an azimuth of 0 degrees and an elevation of 20 degrees.

Figure 12 is an iso-power contour plot for a null formed at zero azimuth and elevation. The elongation of the iso-power contours is very apparent in this example. The ratio of the angular extent of the contours in the elevation direction to the azimuth direction is about 4.0; interestingly, this compares well with the corresponding value of 4.5 for the ratios of the mutual coupling (S_{12}) coefficients between adjacent elements (see Table 1). The shape of the iso-power contours

could be made more circular by using elements having equal coupling in the E- and H-planes (e.g., by using square elements).

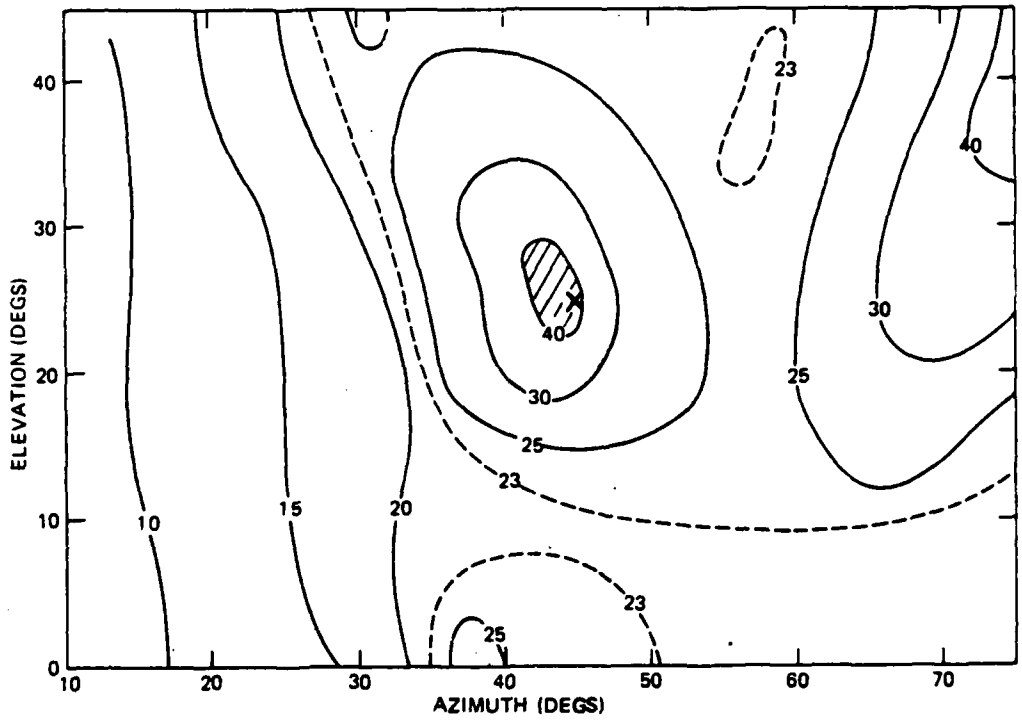

FIGURE 9. Pattern Contour Plot for Adapted Pattern. Contours are in decibels below main lobe response. The cross indicates direction of jammer during null formation.

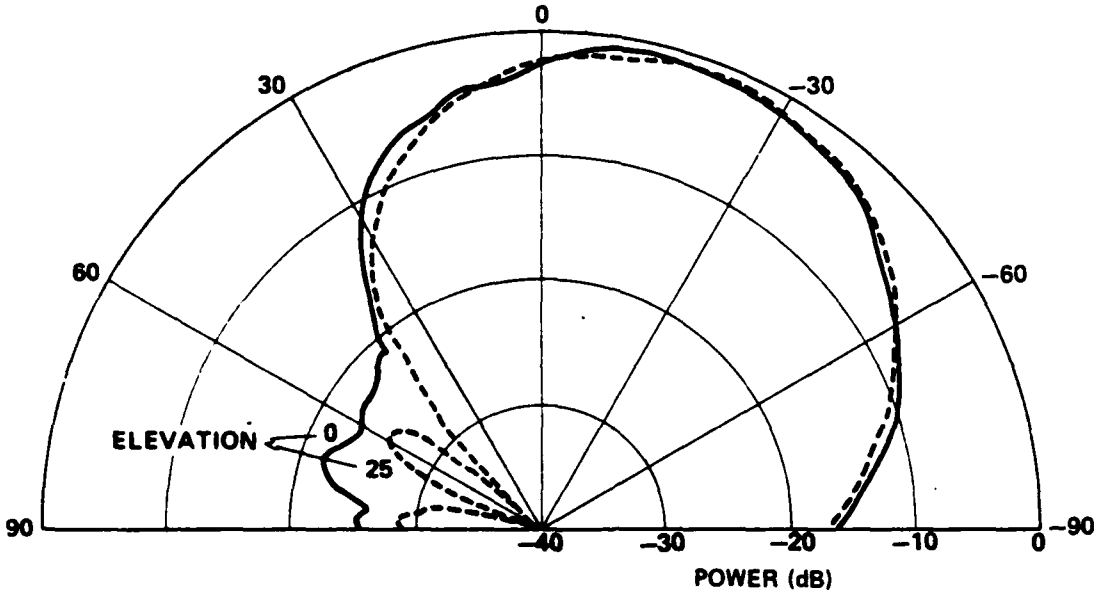

FIGURE 10. Antenna Patterns. The azimuth angle is the polar variable, with patterns plotted for two elevations. A radial value of 0 dB corresponds to a gain of 7.0 dB relative to an isotropic antenna.

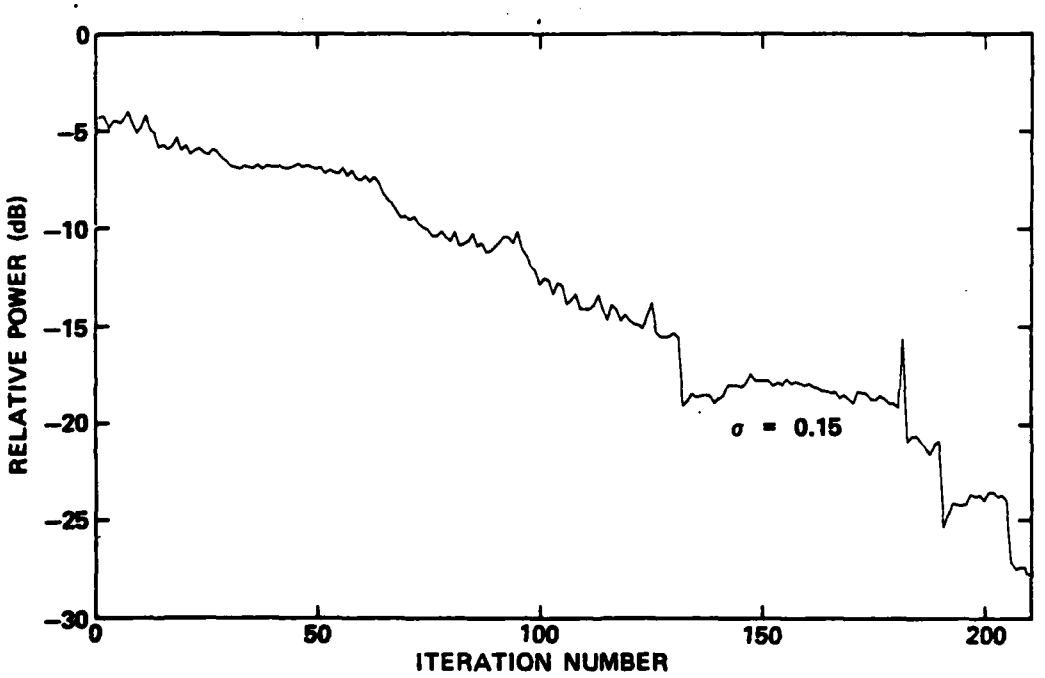

FIGURE 11. Reduction in Jammer Power During Guided Random Search Processing. Jammer incident at $\phi = 0$, $\theta = 20$ degrees.

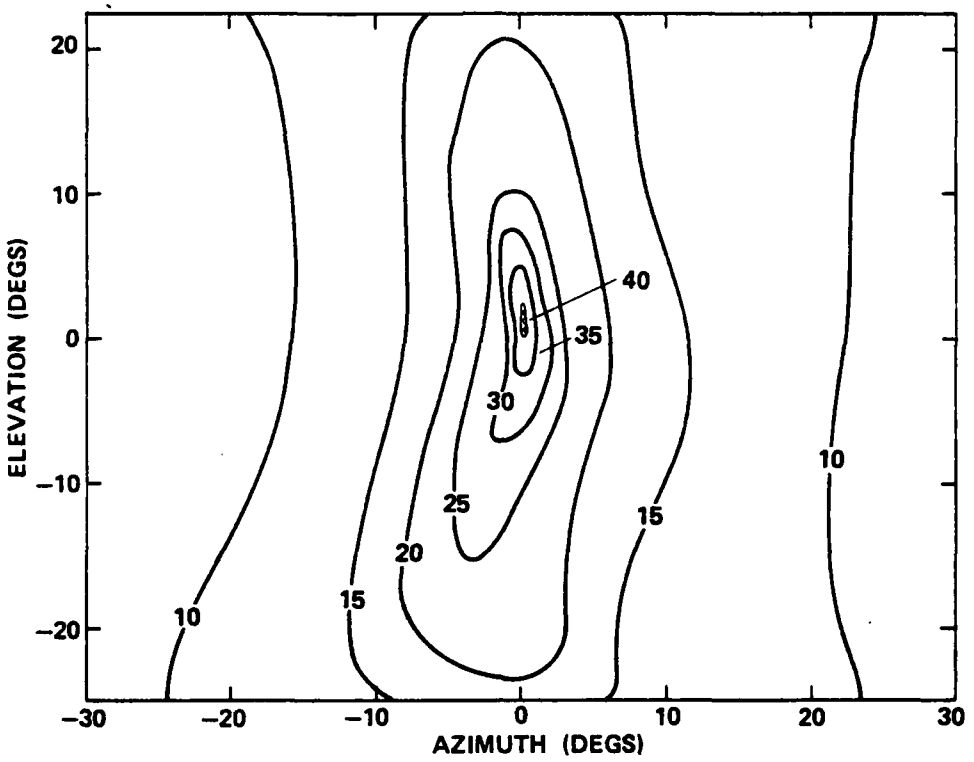

FIGURE 12. Pattern Contour Plot for Jammer Incident at ϕ = 0 Degrees and θ = 0 Degrees.

CONCLUSIONS

The reactively steered adaptive array (RESAA) technique has been extended from a linear array to a planar array and has demonstrated an ability to steer nulls in azimuth and elevation. The guided random search method offers a means of rapid control of a large number of reactively loaded parasitic elements. A null with a depth of 30 decibels relative to the main lobe could be steered towards a single jammer.

ACKNOWLEDGMENT

We gratefully acknowledge the assistance of J. W. McCammon in the fabrication and testing of the array and the phase shifters. We also thank D. J. Banks for the automatic network analyzer measurements for Table 1.

Appendix

ARRAY FACTOR FOR A REACTIVELY STEERED ARRAY

Consider the array of center-fed dipoles shown in Figure A-1, excited by a jammer with power P incident on the array as indicated. The array factor can be written as follows (Reference 5):

$$F(\theta) = \sum_{n=1}^{N} \{[Z_A + Z_L]^{-1}\}_{np} \, e^{jks(n-p)\cos\theta} \tag{A-1}$$

where $k = 2\pi/\lambda$, $\{-\}_{np}$ denotes the np element of the enclosed matrix, $p = (N+1)/2$ is the index for the center driven element, s is the element spacing, $[Z_A]$ is the array impedance matrix, and $[Z_L]$ is the diagonal matrix of reactive loads given by

$$[Z_L] = \begin{bmatrix} X_{L_1} & & & & & 0 \\ & X_{L_2} & & & & \\ & & \ddots & & & \\ & & & X_{L_{(p-1)}} & & \\ & & & 0 & X_{L_{(p+1)}} & \\ & & & & & \ddots \\ 0 & & & & & X_{L_N} \end{bmatrix} \tag{A-2}$$

where X_{Li} is the reactive load on the ith element. It is also convenient to consider the diagonal elements of $[Z_L]$ as a vector denoted by $\vec{X}$.

There are no properties of the matrix inverse in Equation A-1 that permit it to be expanded or simplified, unfortunately. The array factor equation can be written in a more compact form by defining the vector $\vec{I}$ with the components

$$I_n = \{[Z_A + Z_L]^{-1}\}_{np} \tag{A-3}$$

and the steering vector $\vec{U}$ with the components

$$U_n(\theta) = e^{jks(n-p)\cos\theta} \tag{A-4}$$

Then, Equation A-1 can be written as

$$F(\theta) = \vec{I} \cdot \vec{U} \tag{A-5}$$

In the power inversion mode of operation considered in this report, the nulling algorithm objective is to minimize |F| in Equation A-5 by varying the components of the vector $\vec{X}$.

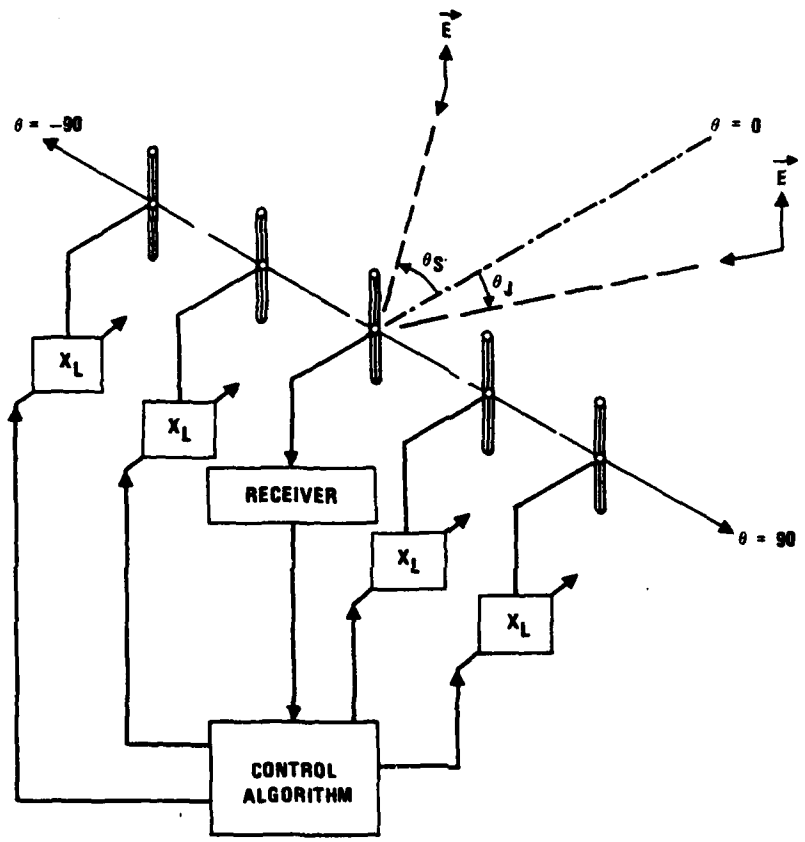

FIGURE A-1. Reactively Steered Antenna Array Geometry.

REFERENCES

1. I. J. Gupta and A. A. Ksienski. "Effect of Mutual Coupling on Performance of Adaptive Arrays," IEEE Trans. Antennas Propag., Vol. AP-31 (September 1983), pp. 785-791.

2. R. F. Harrington. "Reactively Controlled Directive Arrays," IEEE Trans. Antennas Propag., Vol. AP-26 (May 1978), pp. 390-397.

3. Naval Weapons Center. "Reactively Steered Adaptive Array Using Microstrip Patch Elements at 4 GHz," by R. J. Dinger. China Lake, Calif., NWC, February 1983. 34 pp. (NWC TP 6421, publication UNCLASSIFIED.)

4. ------. "Closed-Loop Adaptive Control of a 4.0 GHz Reactively Steered Microstrip Array: Experimental Results," by R. J. Dinger. China Lake, Calif., NWC, October 1983. 22 pp. (NWC TP 6481, publication UNCLASSIFIED.)

5. ------. "A Simulation Study of Jammer Nulling Trade-Offs in a Reactively Steered Adaptive Array," by R. J. Dinger. China Lake, Calif., NWC (in progress). (NWC TP 6611, publication UNCLASSIFIED.)

6. R. J. Dinger. "Reactively Steered Adaptive Array Using Microstrip Patch Elements at 4 GHz," IEEE Trans. Antennas Propag., Vol. AP-32 (1984), pp. 848-856.

7. G. A. Bekey and W. J. Karplus. Hybrid Computation. New York, Wiley, 1968.

INITIAL DISTRIBUTION

8 Naval Air Systems Command
- AIR-03D, G. Heiche (1)
- AIR-330B, F. J. Lueking (1)
- AIR-330D, C. Caposell (1)
- AIR-330E, A. Glista (1)
- AIR-330R, J. Willis (1)
- AIR-340R, J. Smith (1)
- AIR-7226 (2)

5 Chief of Naval Operations
- OP-0941 (1)
- OP-0944 (1)
- OP-098 (1)
- OP-0986 (1)
- OP-987 (1)

8 Chief of Naval Research, Arlington
- ONR-200 (1)
- ONR-210B, LCDR T. L. Swafford (1)
- ONR-250, CDR D. S. Siegal (1)
- ONR-414
  - D. Lewis (1)
  - R. Madan (1)
  - J. Wright (1)
- ONR-430, A. M. Diness (1)
- K. Davis (1)

4 Naval Electronic Systems Command
- Code 61A (1)
- Code 611, B. Hughes (1)
- Code 614, J. Cauffman (1)
- PME-109-20, R. Eisenberg (1)

5 Naval Sea Systems Command
- SEA-003 (1)
- SEA-09B312 (2)
- SEA-62R1
  - C. E. Jedrey (1)
  - T. Tasaka (1)

1 Commander in Chief, U.S. Pacific Fleet (Code 325)

1 Commander, Third Fleet, Pearl Harbor

1 Commander, Seventh Fleet, San Francisco

2 Naval Academy, Annapolis (Director of Research)

3 Naval Air Development Center, Warminster
- A. T. Cerino (1)
- H. H. Heffner (1)
- G. T. Pirrung (1)

1 Naval Ocean Systems Center, San Diego (P. Hansen)

8 Naval Research Laboratory
  Code 7500, J. R. Davis (1)
  Code 7550
    D. Himes (1)
    W. Meyers (1)
    L. Wagner (1)
  W. Gabriel (1)
  F. F. Kretschmer (1)
  C. M. Krowne (1)
  D. Townsend (1)
3 Naval Ship Weapon Systems Engineering Station, Port Hueneme
  Code 5711, Repository (2)
  Code 5712 (1)
1 Naval War College, Newport
1 Office of Naval Technology, Arlington (MAT-073)
1 Army Research Office, Research Triangle Park (J. W. Mink)
1 Harry Diamond Laboratories, Adelphi (A. .R. Sindoris)
1 Air Force Intelligence Service, Bolling Air Force Base (AFIS/INTAW, Maj. R. Lecklider)
2 Rome Air Development Center, Griffiss Air Force Base
  DCCR, J. A. Graniero (1)
  OCTS, V. Vannicola (1)
2 Rome Air Development Center, Hanscom Air Force Base
  R. Mailloux (1)
  H. Steyskal (1)
12 Defense Technical Information Center
1 General Atronics Corporation, Philadelphia, PA (L. R. Burgess)
3 Lincoln Laboratory, MIT, Lexington, MA
  J. T. Mayhan (1)
  K. Senne (1)
  A. Simmons (1)
1 New Mexico State University, Physical Science Laboratory, Las Cruces, NM (K. R. Carver)
2 Ohio State University, ElectroScience Laboratory, Columbus, OH
  R. T. Compton (1)
  A. A. Ksienski (1)
1 R. C. Hansen, Inc., Tarzana, CA (R. C. Hansen)
1 Stanford University, Department of Electical Engineering, Stanford, CA (B. Widrow)
1 Syracuse University, Department of Electrical and Computer Engineering, Syracuse, NY (R. A. Harrington)
2 University of California, Electrical Sciences and Engineering Department, Los Angeles, CA
  N. G. Alexopoulos (1)
  R. S. Elliott (1)
1 University of Colorado, Electromagnetics Laboratory, Boulder, CO (D. C. Chang)
1 University of Houston, Department of Electrical Engineering, Houston, TX (S. A. Long)
1 University of Pennsylvania, Moore School of Electrical Engineering, Philadelpia, PA (B. D. Steinberg)
1 University of Southern California, Department of Electrical Engineering (Systems), Los Angeles, CA (L. Griffiths)
1 Zeger-Abrams, Inc., Glenside, PA (A. E. Zeger)

END

FILMED

8-85

DTIC